



HAL
open science

New CCD Astrometric Observations of Himalia Using Gaia DR2 in 2015-2021

Y. J. Shang, Q. Y. Peng, Z. J. Zheng, A. Vienne, B. F. Guo, F. R. Lin, Y. Chen

► **To cite this version:**

Y. J. Shang, Q. Y. Peng, Z. J. Zheng, A. Vienne, B. F. Guo, et al.. New CCD Astrometric Observations of Himalia Using Gaia DR2 in 2015-2021. *The Astronomical Journal*, 2022, 163, 10.3847/1538-3881/ac57c0 . insu-03718984

HAL Id: insu-03718984

<https://insu.hal.science/insu-03718984>

Submitted on 11 Jul 2022

HAL is a multi-disciplinary open access archive for the deposit and dissemination of scientific research documents, whether they are published or not. The documents may come from teaching and research institutions in France or abroad, or from public or private research centers.

L'archive ouverte pluridisciplinaire **HAL**, est destinée au dépôt et à la diffusion de documents scientifiques de niveau recherche, publiés ou non, émanant des établissements d'enseignement et de recherche français ou étrangers, des laboratoires publics ou privés.



Distributed under a Creative Commons Attribution 4.0 International License



New CCD Astrometric Observations of Himalia Using Gaia DR2 in 2015–2021

Y. J. Shang^{1,3}, Q. Y. Peng^{1,3} , Z. J. Zheng^{1,3}, A. Vienne^{2,3}, B. F. Guo^{1,3}, F. R. Lin^{1,3,4}, and Y. Chen^{1,3}

¹Department of Computer Science, Jinan University, Guangzhou 510632, People's Republic of China
²IMCCE, Observatoire de Paris, UMR 8028 du CNRS, Sorbonne Université, Université de Lille, 77 av. Denfert-Rochereau, F-75014 Paris, France

³Sino-French Joint Laboratory for Astrometry, Dynamics and Space Science, Jinan University, Guangzhou 510632, People's Republic of China

⁴School of Software, Jiangxi Normal University, Nanchang 330022, People's Republic of China

Received 2022 January 14; revised 2022 February 18; accepted 2022 February 21; published 2022 April 12

Abstract

The long arc and high-quality astrometric measurements of outer irregular satellites are prerequisites for improving their orbital theories and increasing the precision of their ephemerides. In order to obtain good astrometric positions of Himalia, the largest irregular satellite of Jupiter, we have processed and reduced 911 ground-based CCD frames obtained between 2015 and 2021 by three telescopes (including 1 and 2.4 m telescopes at Yunnan Observatory, and 0.8 m telescope at Purple Mountain Observatory) over 61 nights. Subtracting off the companion star of our target by constructing an effective point-spread function (ePSF) model in some CCD frames, the ePSF-subtracted technique is used to reduce the centering error. Some additional techniques are applied in data reduction to further improve positional accuracy and precision of Himalia. This includes geometric distortion correction, weighted polynomial plate models, and the precision-premium effect, since their relative positional measurements have better precision when two objects are very near (e.g., less than 60"). The star catalog Gaia DR2 is used for astrometric calibration, and theoretical positions of Himalia are retrieved from JPL Horizons ephemeris, including the satellite ephemeris Jup344 and the newest planetary ephemeris DE441. Our results show the mean ($O - C$)s (observed minus computed) of the positional residuals of Himalia are $-0.''004$ and $0.''005$ in R.A. and decl., respectively, and their corresponding standard deviations are about $0.''020$ in each direction.

Unified Astronomy Thesaurus concepts: [Observational astronomy \(1145\)](#); [Astronomical techniques \(1684\)](#)

1. Introduction

Outer irregular satellites of major planets are usually more distant, highly eccentric, inclined orbits than their regular ones (Grav et al. 2015), and they are subject to strong perturbations from the Sun due to their large semimajor axes (Emelyanov 2010), which are interesting targets for astrometric research. Matters relating to the planetology and orbital dynamics of the distant outer satellites families of giant planets attach great importance to the fundamental problems of the solar system research (Frouard et al. 2011; Khovritchev et al. 2015). Their dynamical properties can provide a window into the capture mechanisms, predicting occultation events, and the role that resonances played in orbital stability and the long-term chaotic diffusion of the different families of satellites (Nesvorný et al. 2003; Brozović & Jacobson 2017). The best way to obtain their physical parameters, which is important for studying the origin of them and how they were captured, is for the orbits to be well known (Gomes-Júnior et al. 2015). Knowledge of satellites can also in turn provide an important clue to understanding how the giant planets formed, and deducing positions of their planets indirectly (Robert et al. 2011). Continuous highly precise astrometric observations for accurate positions covering long-term intervals with a high density are an effective way to make progress in improving ephemerides (Emelyanov 2010), contributing to studies in the dynamic characteristics (Arlot et al. 2012) and supporting relevant deep-space exploration missions of satellites.

Jupiter has 59 known irregular satellites, and Himalia, which was discovered by Charles D. Perrine at Lick Observatory in 1904 (Perrine 1905) and observed with disk-resolved images in a spacecraft by the Cassini ISS in 2000 (Porco et al. 2003), is the largest member. It orbits Jupiter in a prograde orbit with a mean inclination of $\sim 28^\circ$ and in a period of 250.56 days, as well as a semimajor axis of 11.5 million km (or ~ 165 Jupiter radii) belonging to a distant outer satellite of Jupiter (Grav et al. 2015). Grav et al. (2003) show that the satellites of the Jovian Prograde Group Himalia are all clustered in the gray color class implying that they have surfaces similar to that of C-type asteroids. Himalia's low thermal inertia and surface roughness (Grav et al. 2015) result in a dark apparent magnitude, and the albedo of visible light is about $(5.7 \pm 0.8)\%$. These physical characteristics lead to the increasing difficulty of obtaining its high-precision ground-based observations.

Astrometric positions of Himalia have been measured using a variety of star catalogs in the past (e.g., Stone 2001; Gomes-Júnior et al. 2015; Khovritchev et al. 2015; Peng et al. 2017; Yan et al. 2019), and previous work has shown that systematic errors in star catalogs can affect the accuracy of astrometric observations (Eggl et al. 2020). We use Gaia DR2 (Gaia Collaboration et al. 2018a, 2018b) released in 2018 April by the European Space Agency, which has become the well-known standard for minor planet astrometry, as the reference star catalogs to obtain much higher positional accuracy of Himalia. Gaia DR2's uniformity and high quality in both stellar positions and proper motion have been used as a reference to calculate debiasing tables for 26 astrometric catalogs (Eggl et al. 2020). Our observations, ranging from 2015 to 2021 taken with different telescopes at three sites, have an opportunity to constrain the observed systematic errors caused by the instruments and the weather conditions. Moreover, we

Table 1
Instrumental Details for Telescopes and CCD Detectors

Parameters	2.4 m	1 m	0.8 m
Approximate focal length	1920 cm	1330 cm	800 cm
Diameter of primary mirror	240 cm	100 cm	80 cm
CCD field of view (effective)	$9' \times 9'$	$7' \times 7'$ (2015–2020) $16' \times 16'$ (2021)	$11' \times 11'$
Size of CCD array (effective)	1900×1900	2048×2048 (2015–2020) 4096×4112 (2021)	2048×2048
Size of pixel	$13.5 \mu \times 13.5 \mu$	$13.5 \mu \times 13.5 \mu$ (2015–2020) $15 \mu \times 15 \mu$ (2021)	$13.5 \mu \times 13.5 \mu$
Approximate scale factor	$0''.286 \text{ pixel}^{-1}$	$0''.209 \text{ pixel}^{-1}$ (2015–2020) $0''.234 \text{ pixel}^{-1}$ (2021)	$0''.346 \text{ pixel}^{-1}$

Table 2
Observations for Open Cluster (Calibration Fields) and Himalia (Target) Corresponding to the Observational Year

Obs Years	Calibration Fields	No. Frame (nights)	Himalia no. Frame (nights)	Himalia ZD (mean) (deg)	Telescope
2015	M 35	111(2)	27(2)	9–18(13.5)	1 m
2016	M 35	275(6)	177(7)	20–34(26)	1 m
2017	M 67	100(2)	176(5)	31–47(39.4)	1 m
2017	NGC 6633	44(1)	45(3)	48–50(49)	2.4 m
2018			77(8)	41–44(42.3)	1 m
2018			27(4)	45–49(47)	2.4 m
2019			93(6)	48–49(48.5)	1 m
2019			28(4)	59–60(59)	0.8 m
2019			64(6)	49–52(50.3)	2.4 m
2020			32(2)	50–59(54.5)	1 m
2020			53(6)	47–48(47)	0.8 m
2021			49(3)	49–51(50)	1 m
2021			63(5)	47–49(48)	2.4 m
Total		530(11)	911(61)		

Note. “No.” and “Himalia no.” are the number of observed frames and observation nights (in parenthesis) of calibration fields and Himalia, respectively. “Himalia ZD” denotes zenith distances ranges and their means (in parenthesis).

take geometric distortion (called GD hereafter) and precision-premium effect into account for accurate positional measurement of Himalia, especially for lots of sparse fields in the period from 2015 to 2017. In this paper, the positional measurement and reduction procedure are based on our own developed software (Peng & Zhang 2006; Peng et al. 2008).

The contents of this paper are arranged as follows. The CCD observations, image-processing techniques and details of reduction are described in Section 2. Section 3 presents the results of data reduction and comparison with different ephemerides. Finally, the conclusions are drawn in the last section.

2. Observations and Reductions

2.1. CCD Observations

Our observations consist of 911 optical CCD frames for Himalia and 530 CCD calibration frames taken with different telescopes and detectors during 7 yr (2015–2021). The observations are made at three sites over 61 nights by our group. Identified are 911 observations of Himalia, with 631 from the 1 m telescope at the Kunming Station (IAU code 286, longitude E $102^\circ 47' 18''$, latitude N $25^\circ 1' 46''$), 199 from the Yunnan Faint Object Spectrograph and Camera instrument attached to the 2.4 m telescope at the Lijiang Station (IAU code O44, longitude E $100^\circ 1' 51''$, latitude N $26^\circ 42' 32''$) of Yunnan Astronomical Observatory and 81 from the 0.8 m telescope at

the Yaoan Station (IAU code O49, longitude E $101^\circ 10' 51''$, latitude N $25^\circ 31' 43''$) of Purple Mountain Observatory. The specifications of instrument and image characteristics are described in Table 1. Noted that, the former CCD with a resolution of 2048×2048 attached to the 1 m telescope is replaced by a new CCD with a resolution of 4096×4112 since 2021.

Table 2 summarizes distributions of the observations with respect to observational year. All the observations are taken through Johnson *I*-type filter and observational zenith distances are smaller than 60° . According to Stone (2002) and Lin et al. (2020), such conditions render differential color refraction negligible in most astrometric applications. The exposure times range from 20 to 120 s, depending on weather conditions. The GD patterns are derived from CCD calibration frames of nearest dates, which are taken by the dithered observational schemes (“+” or “#” type; see Peng et al. 2012). There are less than 15 reference stars in lots of sparse fields in the period from 2015 to 2017, while there are adequate reference stars in dense fields obtained from 2018 to 2021. Depending on the number of field stars, different astrometric reduction schemes are adopted, which will be specified in Section 2.3.

2.2. Image Processing

All frames are preprocessed with bias and flat-field corrections. Noted that, the CCD frames obtained from the

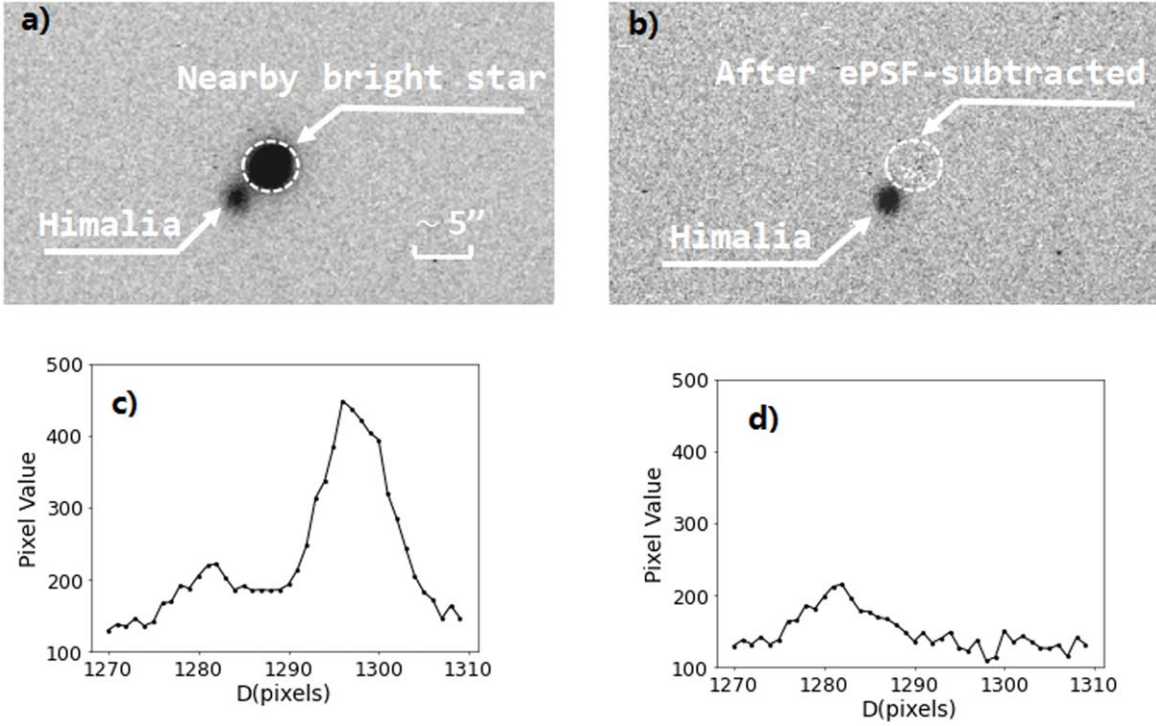


Figure 1. Typical CCD frames of Himalia and its nearby star, as obtained with 1 m telescope of the Yunnan Observatory on 2015 February 14. Upper-left (right) panel: CCD frame before (and after) the ePSF-subtracted technique. Lower-left (right) panel: a slice of the Himalia image that links through the centers of Himalia and nearby star and the same slice after the ePSF-subtracted technique.

2.4 m telescope are clipped into 1900×1900 pixels² to remove the ineffective boundaries. Next, the pixel positions of all stars in each CCD frame are determined with two-dimensional Gaussian-fit centering algorithm. Lastly, we recognize catalog stars and match all pixel positions of fields stars with Gaia DR2 by means of our developed technique (Ren & Peng 2010), considering their proper motions and gnomonic projection effects. It is noted that only reference stars evenly surrounding Himalia are selected to interpolate Himalia’s position to avoid extrapolation errors.

Sometimes, the Himalia image is so near to a brighter star that its center is shifted toward the neighbor star using a two-dimensional Gaussian fit when a small round area is chosen. Therefore, we investigate two processing techniques. One is to adopt double Gaussian-fit centering technique. Specifically, it is a parametric approach that requires a solution for seven parameters expressed by the following Equation (1), where R is regarded as a constant in terms of the rms half width of the image ($1 \text{ FWHM} \approx 2.36 R$) derived from the brightest star near the processing area in image, and $B, H_1, x_1, y_1, H_2, x_2,$ and y_2 are the parameters to be solved. Another option is to remove Himalia’s background gradient by subtracting off an effective point-spread function (ePSF) model (Anderson & King 2000; Anderson et al. 2008) of its neighbor star before we measure Himalia itself (called ePSF-subtracted hereafter). The ePSF is an empirical model describing what fraction of a star’s light would land in a particular pixel. The ePSF-subtracted technique consists of building ePSF with a few bright reference stars with different pixel phase, then fitting the nearby stellar image and subtracting the image. Figure 1 demonstrates a typical CCD frame and the corresponding slice image of Himalia before and after the ePSF-subtracted technique. The astrometric results

using the two techniques will be given in Section 3.

$$F(x, y) = B + H_1 e^{\frac{(x-x_1)^2 + (y-y_1)^2}{2R^2}} + H_2 e^{\frac{(x-x_2)^2 + (y-y_2)^2}{2R^2}}. \quad (1)$$

2.3. Data Reduction

With insufficient reference stars (<15) for high-order polynomial plate model in some sparse fields during 2015 and 2017, we use the weighted low-order polynomial plate models (e.g., 6 or 12 parameters) and GD solutions for the reduction. Since there are adequate reference stars in dense fields obtained from 2018 to 2021, a weighted high-order polynomial—a 30 parameter plate model is adopted, whose high-order terms absorb the systematic errors caused by all astrometric effects (including GD, differential atmospheric refraction, and differential aberration). More detailed descriptions about the astrometric reduction procedures are explained as follows.

First, in order to reduce the residual errors when using low-order polynomial plate model, we derive an average GD solution based on calibration frames of open clusters, according to the method of Peng et al. (2012). The two typical GD patterns for the 1 m and 2.4 m telescopes administered by Yunnan Observatories are shown in Figure 2. It can be seen that, the maximum GD of 1 m telescope reaches 0.42 pixels (~ 88 mas), and the maximum GD of 2.4 m telescope reaches 2.46 pixels (~ 704 mas). Second, we derive the standard coordinates of reference stars via the central projection (Green 1985), and adopt the weighted polynomial plate model to relate standard coordinates to their pixel coordinates, which are described in detail in Lin et al. (2019). Based on the solved parameters of polynomial plate model (and GD solution if needed), we calculate Himalia’s observed astrometric positions.

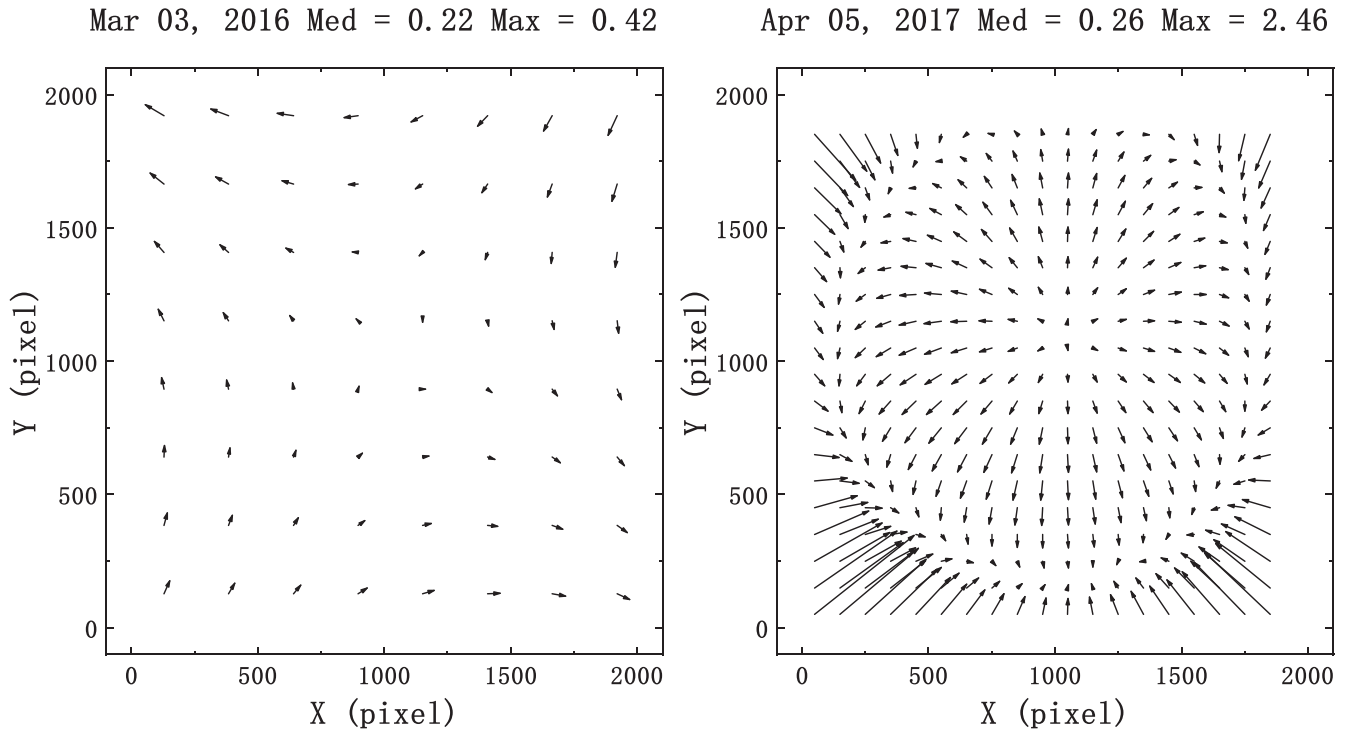


Figure 2. Typical GD patterns derived from a Johnson *I*-type filter from observations of M35 taken with 1 m telescope at Kunming Station and NGC6633 taken with 2.4 m telescope at Lijiang Station on two nights. At the top of each panel, the observational date, the median and maximum GD values are listed in units of pixels. A factor of 200 is used to exaggerate the magnitude of each GD vector.

Additionally, considering the precision-premium effect on a short-separation star pair (Lin et al. 2019) could be used to improve our results, we also adopt an alternative technique to calculate Himalia’s observed astrometric positions, when the separation between Himalia and an isolated high signal-to-noise ratio (S/N) star is less than $60''$. According to Lin et al. (2019), bright neighbors used as references will have a good internal precision, since the systematic errors of the references and the target are similar.

Finally, compared with Himalia’s theoretical astrometric positions from the JPL⁵ Horizons ephemeris (Chamberlin et al. 1997), including the satellite ephemeris Jup344 and planetary ephemeris DE441 (Jup344+DE441), the positional residuals (observed minus computed; $O - C$ s) of Himalia are estimated from the offsets, and the standard deviations (SDs) of all data sets could be obtained.

3. Results and Discussion

The image-processing and data-reduction techniques are essential to obtain highly precise astrometric results, which will be described in the following two aspects. Firstly, for the frames where the object is too close to its companion star, double Gaussian-fit and ePSF-subtracted techniques are used to improve the centering accuracy and precision. Secondly, the precision-premium technique is also used to improve the precision for a short separation (i.e., the relative angular distance less than $60''$) between the target and its good-position neighbor star. Additionally, When inadequate Gaia stars for high-order polynomial plate models are taken in the field of view, the weighted low-order plate models (e.g., 6 or 12 parameters) are used after GD correction during the data

reduction (details can be found in our previous researches see Peng et al. 2017; Lin et al. 2019). Our final optimal results applying these mentioned techniques, the comparisons with different ephemerides and previous observations are showed in Section 3.3.

3.1. The Comparison Between Double Gaussian-fit and ePSF-subtracted Techniques

For the three frames taken in Kunming Station on February 14, 2015, where a reference star falls quite near to Himalia, mentioned in Section 2.2, we determine the center of Himalia by using double Gaussian-fit and ePSF-subtracted techniques to reduce the systematic error involved by its nearby star. And we plot the $(O - C)$ residuals for 22 observations in the whole observation night in Figure 3. The two techniques can improve mean offsets of $-0''.7$ in each direction using classical two-dimension Gaussian fit, and of about $-0''.2$ using a double Gaussian fit in comparison with the $(O - C)$ s using the ePSF-subtracted technique. Limited to the number of proper frames here, we will do further research for measuring the target with near neighbors in the future.

3.2. Precision-premium Technique

We find there are 267 CCD frames satisfying our criteria of precision-premium working, outlined in Section 2.3. We compare the results of using the classical procedures and precision-premium technique. Corresponding $(O - C)$ residuals are plotted in Figure 4, in which the black squares are the $(O - C)$ s reduced by classical procedure and the red dots are the results using the precision-premium technique. Table 3 also shows the statistic of reduction results. The standard deviations of classical procedures are $0''.025$ in R.A. and $0''.026$ in decl., and after applying precision-premium technique, the precision

⁵ <https://ssd.jpl.nasa.gov/>

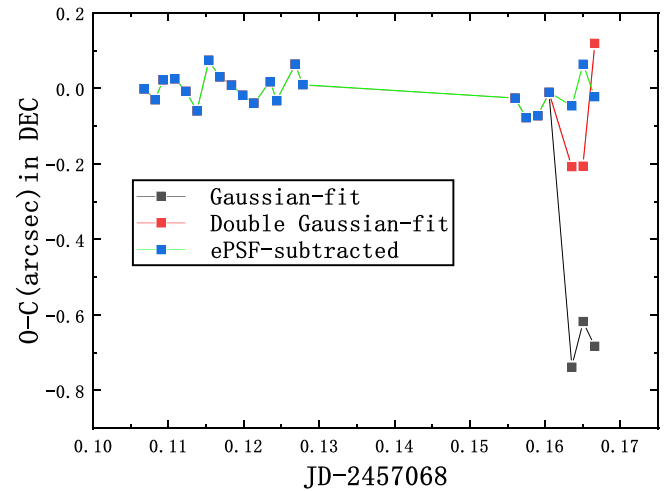
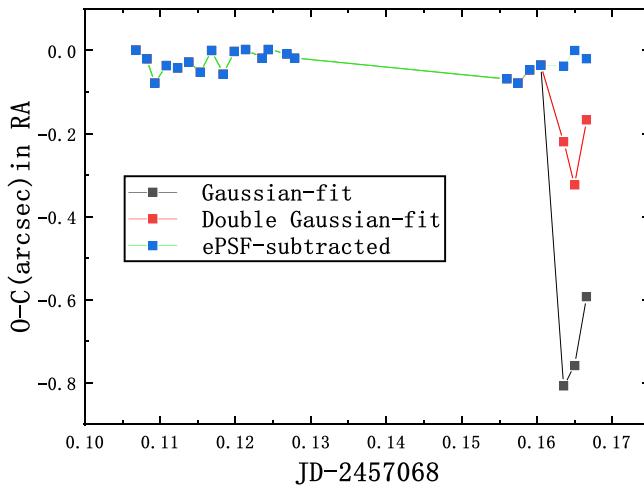


Figure 3. $(O - C)$ residuals of Himalia with different processing techniques. The left and right panels show the results with regard to JD in R.A. and decl., respectively. The black, red, and blue squares represent $(O - C)$ residuals using classical two-dimension Gaussian-fit, double Gaussian-fit, and ePSF-subtracted techniques, respectively.

is improved to $0''.022$ in R.A. and $0''.021$ in decl. Clearly, the improvements of the precision of Himalia in two directions are significant, which demonstrate the potential to achieve higher precision in conventional ground-based astrometry by using precision-premium technique.

3.3. Comparisons with Different Ephemerides and Previous Observations

We use the Gaia DR2 catalog for astrometric calibration, and the derived astrometric positions of Himalia are compared with JPL ephemeris (JUP344+DE441). There are 911 $(O - C)$ s as shown in Figure 5, and the different colored points identify observations for different telescopes. Table 4 lists the results of the mean $(O - C)$ s and their dispersions (i.e., SD). As seen in Table 4, the mean $(O - C)$ s for observations at Yaoan Station fluctuate more greatly in two directions than other two stations, which demonstrates the advantages of large-aperture telescopes in highly precise astrometric position measurements. With the help of image-processing and data-reduction techniques, we compute the formally mean $(O - C)$ s for all data sets are $-0''.004$ and $0''.005$ in R.A. and decl., respectively. Correspondingly, their SDs are estimated about $0''.020$ with good internal convergence.

The results of astrometric observations are valuable only if its accuracy is sufficient to assess significant dynamical effects (Arlot et al. 2012). Intending to check and analyze our results, we also compute $(O - C)$ s with regard to the ephemerides retrieved from the Institut de Mécanique Céleste et de Calcul des Éphémérides (IMCCE)⁶, including the satellite ephemeris Emelyanov’s model (Version 2021-01-31) and planetary ephemeris DE441. Table 5 denotes the statistics of $(O - C)$ residuals of Himalia using both JPL and IMCCE ephemerides, and the corresponding $(O - C)$ residual distributions from two ephemerides are displayed in the scatter plot Figure 6. The slight differences are from the different satellite ephemerides on account of the same planetary ephemeris DE441 used. The mean $(O - C)$ s of Himalia for ephemeris retrieved from IMCCE are $-0''.005$ and $0''.014$ in R.A. and decl., respectively. Correspondingly, their standard deviations are about $0''.024$ and

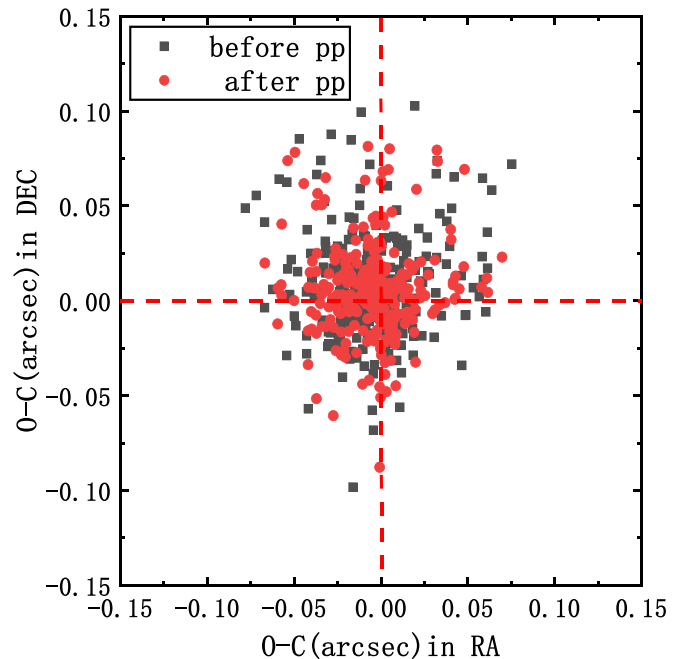


Figure 4. Comparison of dispersion of $(O - C)$ residuals of Himalia in decl. with respect to R.A. before and after precision premium (pp).

Table 3
Statistical Results of Astrometric Reduction before and After Precision Premium (pp)

Methods	No.	$\langle O - C \rangle$	SD in R.A. (arcsec)	$\langle O - C \rangle$	SD in Decl. (arcsec)
before pp	267	-0.005	0.025	0.007	0.026
after pp	267	-0.005	0.022	0.005	0.021

$0''.022$. The $(O - C)$ residuals in decl. and SDs in two directions from IMCCE are slightly greater than JPL. Overall, it shows intuitively that our astrometric positions are in good agreement with the two ephemerides, in terms of accuracy and precision.

Additionally, to compare our observations with previous ones, some major observational statistics of Himalia are listed

⁶ <https://www.imcce.fr/services/ephemerides/>

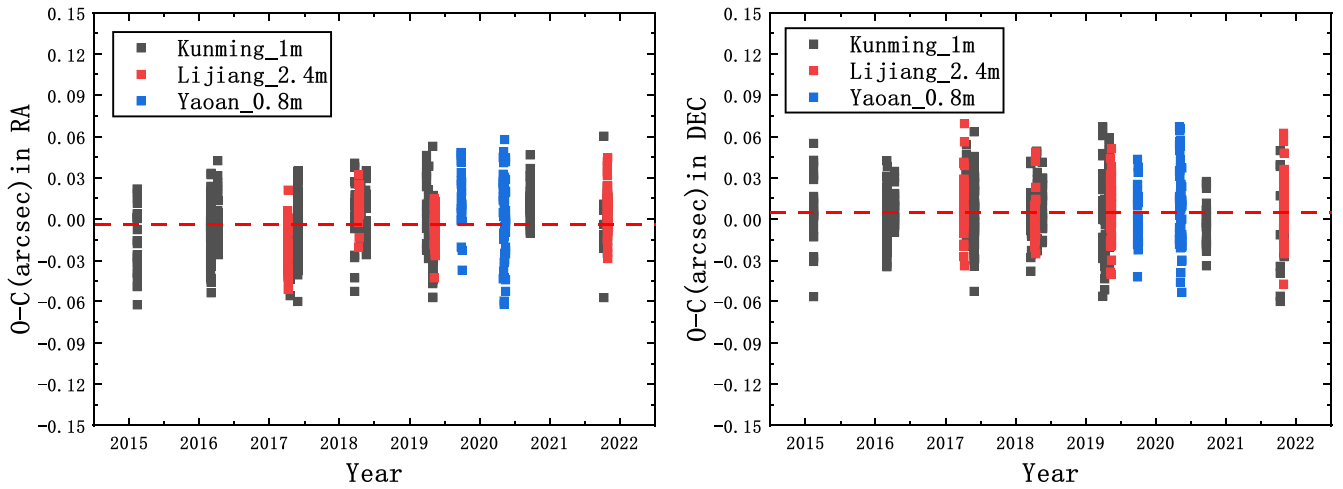


Figure 5. $(O - C)$ residuals of the positional offsets with regard to JPL ephemeris (JUP344+DE441) for Himalia taken by different telescopes during 2015 and 2021. The dark squares are for observations with 1 m telescope from Kunming Station, the red ones for 2.4 m from Yaoan Station and the blue ones for 0.8 m from Lijiang Station in each direction. And the two red dash lines represent mean $(O - C)$ s in each panel.

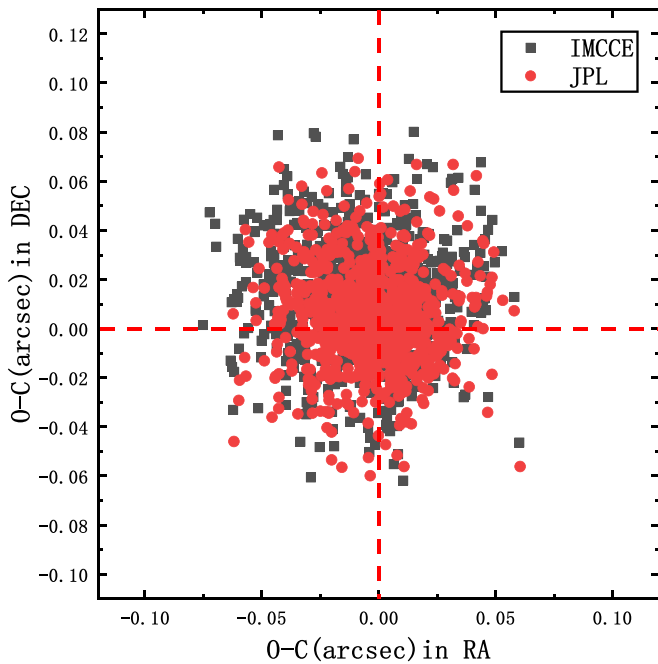


Figure 6. $(O - C)$ residuals of Himalia in decl. with respect to R.A. The dark squares represent the $(O - C)$ residuals for IMCCE and the red points for JPL.

in Table 6. We have obtained some previous astrometric data of Himalia from the Natural Satellites Data Center (NSDC⁷; Arlot & Emelyanov 2009) and calculated the means of $(O - C)$ residuals and standard deviations. The ephemeris used for all the observations is retrieved from JPL. The positions of Himalia are observed topocentric astrometric positions. Our results show that the total accuracy and precision of Himalia are similar to Yan et al. (2019)’s work because of most of observations taken by the same telescope (i.e., 1 m telescope at Kunming Station). It can give proof that catalog Gaia DR2 and our measuring techniques mentioned in this paper have the favorable prospects in enhancing the accuracy and precision of the astrometric observations.

⁷ <http://nsdb.imcce.fr/nsdb/home.html>

Table 4
Statistics on the Astrometric Reduction for Positions of Himalia

IAU Code	Telescope	No.	$\langle O - C \rangle$	SD in R.		SD in
				A.	$\langle O - C \rangle$	Decl.
				(arcsec)	(arcsec)	(arcsec)
286	1 m	631	-0.005	0.020	0.004	0.020
O44	2.4 m	199	-0.002	0.017	0.008	0.020
O49	0.8 m	81	0.005	0.029	0.008	0.027
Total		911	-0.004	0.020	0.005	0.020

Note. “IAU code” and “Telescope” are the codes of observational stations and corresponding aperture of telescope used. “No.” is the number of observations. The following columns list the mean $(O - C)$ s and their SDs in R.A. and decl., respectively.

Table 7 lists an extract of our observed topocentric astrometric positions of Himalia, based on Gaia DR2 catalog and JPL ephemeris (JUP344+DE441). The data are presented in the following form: the IAU code is the code of observatory. JD represents the exposure middle time of each frame in the form of Julian date (UTC). R.A., expressed in hours, minutes, and seconds, is the position of Himalia in R.A. Expressed in degrees, arcminutes, and arcseconds is the position in decl.⁸

4. Conclusions

Aimed to provide new, precise positions of Himalia in a long time span to promote its orbit and ephemeris, we have processed 1441 FITS images (911 Himalia and 530 Calibration Fields for GD solution) and presented 911 topocentric astrometric positions of Himalia, acquired by three telescopes at Yunnan Province between 2015 and 2021 over 61 nights. When less than 15 reference stars are taken in lots of sparse fields in the period from 2015 to 2017, the weighted low-order plate models (e.g., 6 or 12 parameters), after GD correction, are used to fit transformation. While in dense fields obtained from 2018 to 2021, the weighted high-order polynomial plate model (30 parameters) is applied during the data reduction. When Himalia images too near to a high S/N reference star, we use the ePSF-subtracted technique to

⁸ The whole table is available on the website <https://astrometry.jnu.edu.cn/download/list.htm>.

Table 5
Statistics of ($O - C$) Residuals of Himalia in Comparison with JPL and IMCCE

IAU Code	No.	JPL (JUP344+DE441)				IMCCE (Emelyanov's Model+DE441)			
		$\langle O - C \rangle$ R.A. (arcsec)	SD	$\langle O - C \rangle$ Decl. (arcsec)	SD	$\langle O - C \rangle$ R.A. (arcsec)	SD	$\langle O - C \rangle$ Decl. (arcsec)	SD
286	631	-0.005	0.020	0.004	0.020	-0.006	0.024	0.013	0.022
O44	199	-0.002	0.017	0.008	0.020	-0.008	0.023	0.016	0.019
O49	81	0.005	0.029	0.008	0.027	0.005	0.029	0.017	0.028
Total	911	-0.004	0.020	0.005	0.020	-0.006	0.025	0.014	0.022

Note. “IAU code” and “No.” are the observational stations code and number of observations. Columns 3–6 list the mean ($O - C$)s and their SDs derived from JPL in R.A. and decl., respectively, and the following columns list the ones derived from IMCCE.

Table 6
Compared with Previous Observations Downloaded from NSDC

IAU code	Time (Year)	Author	No.	$\langle O - C \rangle$	SD	$\langle O - C \rangle$	SD
				R.A. (arcsec)		Decl. (arcsec)	
689	2013–2015	(Stone 2001)	93	-0.038	0.161	-0.009	0.227
511	1998–2008	(Gomes-Júnior et al. 2015)	357	-0.017	0.047	-0.009	0.062
874	1995–2014	(Gomes-Júnior et al. 2015)	854	-0.016	0.106	-0.007	0.047
T05	2017	Minor Planet Center 103147-103148	32	0.053	0.113	-0.018	0.123
286	2016–2018	(Yan et al. 2019)	267	-0.001	0.021	0.003	0.025
286&O44&O49	2015–2021	Our work	911	-0.004	0.020	0.005	0.020

Note. “IAU code” and “Time” are the IAU code of observatory and the time range of observations. “Author” and “No.” show the author and total amount of CCD observations. The following columns present the mean ($O - C$)s and its standard deviations compared with the ephemeris JPL in R.A. and decl., respectively.

Table 7
Extract of the Observations of Himalia

IAU code	Date (JD)	R.A. (h m s)	Decl. ($^{\circ}$ ' ")
286	2457066.15338889	09 17 30.641	+17 13 45.40
286	2457066.15188194	09 17 30.676	+17 13 45.20
286	2457066.14617477	09 17 30.819	+17 13 44.43
.....
O44	2457849.27308681	13 09 19.832	-05 15 37.23
O44	2457849.27257176	13 09 19.844	-05 15 37.33
O44	2457849.27205903	13 09 19.856	-05 15 37.39
.....
O49	2458985.30939236	19 58 52.667	-21 13 54.51
O49	2458985.30861111	19 58 52.659	-21 13 54.53
O49	2458985.30782523	19 58 52.660	-21 13 54.52

Note. “Date” is the exposure middle time of each CCD observation in the form of JD. “R.A.” and “decl.” are the observed topocentric astrometric positions in R.A. and decl., respectively.

reduce centering error introduced by this neighbor. The precision-premium technique is also used to further achieve the better precision for a small separation ($<60''$) between Himalia and a high S/N reference star.

Based on Gaia DR2 for astrometric calibration, our results present that the mean ($O - C$)s of Himalia are about $-0''.004$ and $0''.005$ compared with ephemerides retrieved from JPL in R.A. and decl., respectively. The corresponding standard deviation are estimated at $0''.020$ in each direction. Compared with the ($O - C$)s derived from IMCCE, our results also show the consistency in both R.A. and decl. Our positional precision of Himalia has been significantly improved compared with the previous observations. We believe that our results would be valuable to improve dynamical models and data calibration of Himalia’s ephemeris.

This work was supported by the National Natural Science Foundation of China (grant Nos. 11873026, 11273014), by the Joint Research Fund in Astronomy (grant No. U1431227) under cooperative agreement between the National Natural Science Foundation of China (NSFC) and Chinese Academy Sciences (CAS), by the China Manned Space Project with NO. CMS-CSST-2021-B08, and partly by the Fundamental Research Funds for the Central Universities and Excellent Postgraduate Recommendation Scientific Research Innovative Cultivation Program of Jinan University. This work has made use of data from the European Space Agency (ESA) mission Gaia (<https://www.cosmos.esa.int/gaia>), processed by the Gaia Data Processing and Analysis Consortium (DPAC; <https://www.cosmos.esa.int/web/gaia/dpac/consortium>). Funding for the DPAC has been provided by national institutions, in particular the institutions participating in the Gaia Multilateral Agreement.

ORCID iDs

Q. Y. Peng  <https://orcid.org/0000-0001-7467-1585>

References

- Anderson, J., & King, I. R. 2000, *PASP*, **112**, 1360
 Anderson, J., Sarajedini, A., Bedin, L. R., et al. 2008, *AJ*, **135**, 2055
 Arlot, J.-E., Desmars, J., Lainey, V., & Robert, V. 2012, *P&SS*, **73**, 66
 Arlot, J. E., & Emelyanov, N. V. 2009, *A&A*, **503**, 631
 Brozović, M., & Jacobson, R. A. 2017, *AJ*, **153**, 147
 Chamberlin, A. B., Yeomans, D. K., Chodas, P. W., et al. 1997, AAS Meeting Abstracts, **29**, 21.06
 Ettl, S., Farnocchia, D., Chamberlin, A. B., & Chesley, S. R. 2020, *Icar*, **339**, 113596
 Emelyanov, N. 2010, *P&SS*, **58**, 411
 Frouard, J., Vienne, A., & Fouchard, M. 2011, *A&A*, **532**, A44
 Gaia Collaboration, Mignard, F., Klioner, S. A., et al. 2018b, *A&A*, **616**, A14
 Gaia Collaboration, Spoto, F., Tanga, P., et al. 2018a, *A&A*, **616**, A13

- Gomes-Júnior, A. R., Assafin, M., Vieira-Martins, R., et al. 2015, *A&A*, **580**, A76
- Grav, T., Bauer, J. M., Mainzer, A. K., et al. 2015, *AJ*, **809**, 809
- Grav, T., Holman, M. J., Gladman, B. J., & Aksnes, K. 2003, *Icar*, **166**, 33
- Green, R. M. 1985, *Spherical Astronomy* (Cambridge: Cambridge Univ. Press)
- Khovritchev, M. Y., Ershova, A. P., Balyaev, I. A., et al. 2015, arXiv:1511.01642
- Lin, F. R., Peng, J. H., Zheng, Z. J., & Peng, Q. Y. 2019, *MNRAS*, **490**, 4382
- Lin, F. R., Peng, Q. Y., & Zheng, Z. J. 2020, *MNRAS*, **498**, 258
- Nesvorný, D., Alvarellos, J. L. A., Dones, L., & Levison, H. F. 2003, *AJ*, **126**, 398
- Peng, H. W., Peng, Q. Y., & Wang, N. 2017, *MNRAS*, **467**, 2266
- Peng, Q. Y., Vienne, A., Wu, X. P., Gan, L. L., & Desmars, J. 2008, *AJ*, **136**, 2214
- Peng, Q. Y., Vienne, A., Zhang, Q. F., et al. 2012, *AJ*, **144**, 170
- Peng, Q. Y., & Zhang, Q. F. 2006, *MNRAS*, **366**, 208
- Perrine, C. D. 1905, *LicOB*, **3**, 129
- Porco, C. C., West, R. A., McEwen, A., et al. 2003, *Sci*, **299**, 1541
- Ren, J. J., & Peng, Q. Y. 2010, *AR&T*, **07**, 115
- Robert, V., de Cuyper, J. P., Arlot, J. E., et al. 2011, *MNRAS*, **415**, 701
- Stone, R. C. 2001, *AJ*, **122**, 2723
- Stone, R. C. 2002, *PASP*, **114**, 1070
- Yan, D., Qiao, R. C., Yu, Y., et al. 2019, *P&SS*, **179**, 104712